

Linear and nonlinear optical properties of one-dimensional photonic crystals containing ZnO defects

Geon Joon Lee^{a),b)} and Young Pak Lee^{a),c)}

Quantum Photonic Science Research Center and Department of Physics, Hanyang University, Seoul 133-791, Korea

Sung Goo Jung and Chang Kwon Hwangbo

Department of Physics, Inha University, Incheon 402-751, Korea

Sunman Kim

Department of Physics, University of Seoul, Seoul 130-743, Korea and Quantum Photonic Science Research Center, Hanyang University, Seoul 133-791, Korea

Inkyu Park

Department of Physics, University of Seoul, Seoul 130-743, Korea

(Received 29 June 2007; accepted 14 August 2007; published online 12 October 2007)

The linear and nonlinear optical properties of one-dimensional photonic crystals containing ZnO defects were studied by linear absorption spectroscopy and the femtosecond *Z*-scan technique. Photonic crystals containing ZnO defects, $(\text{Ta}_2\text{O}_5/\text{SiO}_2)^5/\text{ZnO}/(\text{SiO}_2/\text{Ta}_2\text{O}_5)^5$, were prepared using electron-beam deposition and magnetron sputtering. The transmission spectra of these photonic crystals revealed a defect mode resonance and a broad photonic band gap. The observed transmission spectra could be described by applying the optical transfer matrix formalism to the multilayer structure. When compared with the *Z*-scan curve of the ZnO film, that of the resonant photonic crystal exhibited a larger transmittance dip. The enhancement of the nonlinear absorption in the resonant photonic crystal is due to the strong confinement of the optical field. © 2007 American Institute of Physics. [DOI: [10.1063/1.2787161](https://doi.org/10.1063/1.2787161)]

I. INTRODUCTION

Due to their application in ultraviolet (UV) photonic devices, blue-green laser diodes, and nonlinear optical devices, wide band gap semiconductors have drawn considerable attention in recent years.¹⁻⁷ Among them, ZnO has emerged as a promising optoelectronic material due to its large exciton binding energy of 60 meV, and wide band gap of 3.3 eV. To develop these materials, it is necessary to understand their luminescent mechanism, dephasing dynamics, and optical nonlinearities. Several research groups have studied the photophysical properties of ZnO. Hsieh *et al.* studied the structural and photoluminescence characteristics of ZnO thin films using room temperature sputtering and a rapid thermal annealing process.¹ Huang *et al.* demonstrated room temperature UV lasing in ZnO nanowire arrays.² Cao *et al.* reported the observation of random laser action with coherent feedback in ZnO powder.³ Abrarov *et al.* studied the temperature-dependent photoluminescence characteristics of ZnO embedded in the voids of synthetic opal.⁴ Recently, nanoscaled UV lasers based on ZnO nanostructures have been reported.^{2,5} Although there are many studies on the luminescence and lasing properties of ZnO, little work has been done on its optical nonlinearities. Lin *et al.* studied the optical nonlinearities of ZnO thin films using the femtosecond *Z*-scan technique.⁶ Zhang *et al.* reported the measure-

ment of the third-order optical nonlinearity of ZnO thin films near excitonic resonance using the femtosecond degenerate four-wave-mixing technique.⁷ The enhancement of optical nonlinearities in ZnO is important in practical applications such as optical limiting devices and all-optical switching elements. Therefore, it would be beneficial to study the enhancement of optical nonlinearity in ZnO.

In this study, we used the ZnO defect-containing one-dimensional photonic crystals to enhance nonlinear optical effects. ZnO defect-containing photonic crystals, were $(\text{Ta}_2\text{O}_5/\text{SiO}_2)^5/\text{ZnO}/(\text{SiO}_2/\text{Ta}_2\text{O}_5)^5$, prepared using electron-beam (e-beam) deposition and magnetron sputtering. The linear and nonlinear optical properties of ZnO defect-containing photonic crystals were measured using linear absorption spectroscopy and the femtosecond *Z*-scan technique. The linear optical properties were analyzed using an optical transfer matrix formalism. The nonlinear optical properties were described using the spatial distribution of the squared field strength inside the multilayer structure. The linear and nonlinear optical properties of the ZnO defect-containing photonic crystals were compared with those of ZnO film.

II. EXPERIMENT

One-dimensional photonic crystals containing ZnO defects were designed such that the defect mode resonance could be produced near a wavelength of 800 nm. In order to study the linear and nonlinear optical properties of ZnO, a 210 nm thick ZnO film was deposited onto fused quartz by

^{a)}Author to whom correspondence should be addressed.

^{b)}Electronic mail: glee@hanyang.ac.kr

^{c)}Electronic mail: yplee@hanyang.ac.kr

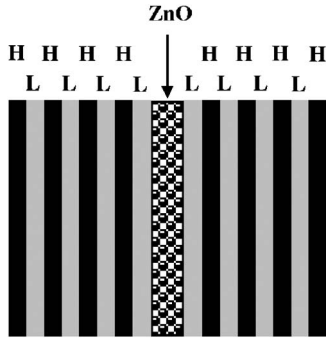


FIG. 1. Geometry of the ZnO-defect-containing photonic crystal. (*H*, high index layer; *L*, low index layer; ZnO, defect layer.)

magnetron sputtering. To enhance nonlinear optical properties with the microcavity effect, photonic crystals containing ZnO defects, $(\text{Ta}_2\text{O}_5/\text{SiO}_2)^5/\text{ZnO}/(\text{SiO}_2/\text{Ta}_2\text{O}_5)^5$, were prepared (Fig. 1). First, a $(\text{SiO}_2/\text{Ta}_2\text{O}_5)^5$ stack was deposited onto a glass plate by alternatively evaporating SiO_2 and Ta_2O_5 using an e-beam method. Next, a ZnO defect layer was deposited onto the $(\text{SiO}_2/\text{Ta}_2\text{O}_5)^5/\text{glass}$. Finally, a $(\text{Ta}_2\text{O}_5/\text{SiO}_2)^5$ stack was deposited onto the $\text{ZnO}/(\text{SiO}_2/\text{Ta}_2\text{O}_5)^5$. The thicknesses of the defect layer, the low-refractive index layer, and the high-refractive index layer were adjusted so that the resonance wavelength of the defect mode and the center of the photonic band gap were located near 800 nm: $\lambda_{\text{peak}}(\text{sample A})=800$ nm and $\lambda_{\text{peak}}(\text{sample B})=810$ nm. The existence of a defect mode and a photonic band gap in the defect-containing photonic crystals were investigated by measuring the optical transmission spectra. The transmission spectra of the films were measured over wavelengths ranging from UV to near-infrared (NIR) using a UV-visible-NIR spectrophotometer (Varian, Cary 500). The nonlinear optical properties of the defect-containing photonic crystals were investigated using the Z-scan technique.⁸ The Z-scan experiment was performed using 130 fs-laser pulses with a wavelength of 800 nm, a repetition rate of 1kHz, and a maximum pulse-energy of 1 mJ.

III. RESULTS AND DISCUSSION

Figures 2(a) and 2(b) show the transmission spectra of the ZnO defect-containing photonic crystals. Figure 2(d) shows the transmission spectrum of a single 210 nm thick film of ZnO. The oscillatory behavior of the transmission spectrum in Fig. 2(d) is due to the interference of the waves reflected from the front and back surfaces of the film. Although this transmission spectrum does not show a particular transmission band, the transmission spectra of the defect-containing photonic crystals [Figs. 2(a)–2(c)] exhibit a defect mode resonance and a broad photonic band gap. The defect mode resonance occurs near 800 nm: $\lambda_{\text{peak}}(\text{sample A})=800$ nm and $\lambda_{\text{peak}}(\text{sample B})=810$ nm. The bandwidths of the two defect mode are ~ 7.3 nm. To understand the underlying physics of the defect mode resonance, we performed a numerical simulation of the transmission spectra of multilayer structures. According to the optical transfer matrix formalism, the transmittance, T_{PC} , of the multilayer stack is given by^{9,10}

$$T_{PC} = \left| \frac{2p_a}{p_a M_{11} + p_a p_s M_{12} + M_{21} + p_s M_{22}} \right|^2. \quad (1)$$

Here, the subscripts in p_a and p_s represent incident medium (air) and substrate. In Eq. (1), the matrix elements of the multilayer stack are obtained from the overall transfer matrix M as follows:

$$M = \begin{pmatrix} M_{11} & M_{12} \\ M_{21} & M_{22} \end{pmatrix} = \prod_{j=1}^N M_j. \quad (2)$$

If the j th layer is characterized by the refractive index, n_j , the extinction coefficient, κ_j , and the thickness, d_j , then the individual transfer matrix, M_j , is given by

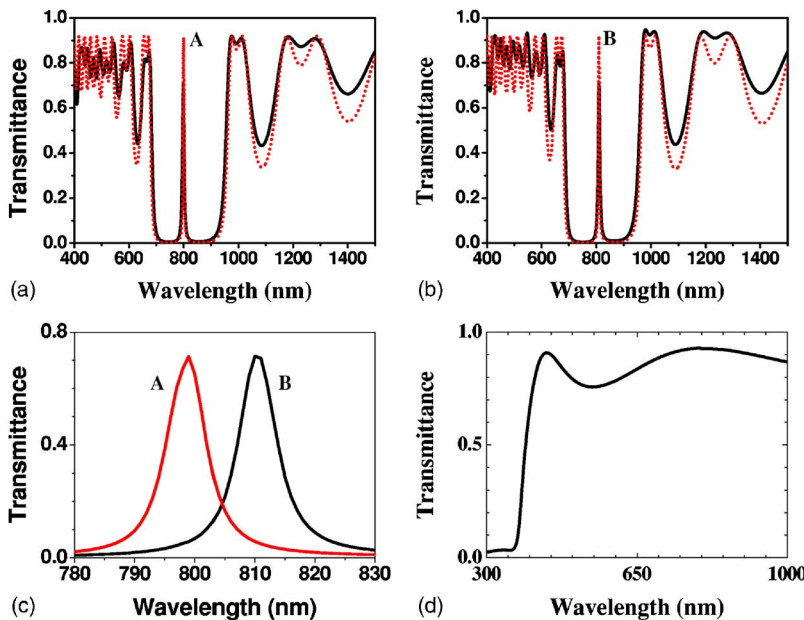


FIG. 2. (Color online) Transmission spectra of (a), (b), and (c), the ZnO-defect-containing photonic crystals, and (d), 210 nm thick ZnO film: (a) $(\text{Ta}_2\text{O}_5/\text{SiO}_2)^5/\text{ZnO}(210 \text{ nm})/(\text{SiO}_2/\text{Ta}_2\text{O}_5)^5$ (sample A), (b) $(\text{Ta}_2\text{O}_5/\text{SiO}_2)^5/\text{ZnO}(219 \text{ nm})/(\text{SiO}_2/\text{Ta}_2\text{O}_5)^5$ (sample B). The expanded view of (a) and (b) over wavelengths from 780 to 830 nm is shown in (c). The solid and dotted lines in the transmission spectra are the experimental and theoretical values, respectively. In the calculated spectra, $n(\text{Ta}_2\text{O}_5)=2.086$, $n(\text{SiO}_2)=1.453$, $n(\text{ZnO})=1.932$, $d(\text{Ta}_2\text{O}_5)=95$ nm, $d(\text{SiO}_2)=137$ nm, $d(\text{ZnO})=(\text{a})210$ nm/ $(\text{b})219$ nm.

$$M_j = \begin{bmatrix} \cos\left(\frac{2\pi}{\lambda} p_j d_j\right) & i \frac{1}{p_j} \sin\left(\frac{2\pi}{\lambda} p_j d_j\right) \\ ip_j \sin\left(\frac{2\pi}{\lambda} p_j d_j\right) & \cos\left(\frac{2\pi}{\lambda} p_j d_j\right) \end{bmatrix}, \quad (3)$$

where

$$p_j = N_j \cos \theta_j.$$

Here $N_j = n_j - i\kappa_j$ is the complex refractive index of the j th layer and θ_j is the angle of incidence for the j th layer. The optical constants used in the calculation of the transmission spectra were obtained with the spectroscopic ellipsometry.

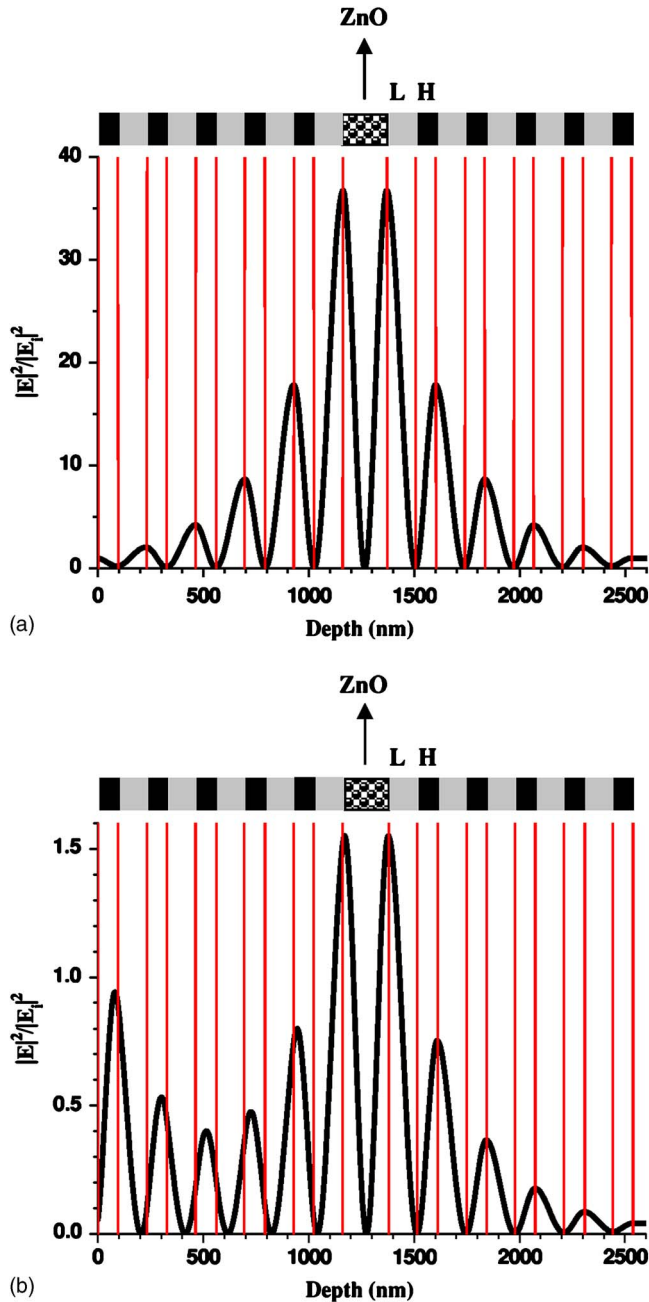


FIG. 3. (Color online) Spatial distribution of the squared field strength inside the ZnO-defect-containing photonic crystals: (a) $(\text{Ta}_2\text{O}_5/\text{SiO}_2)^5/\text{ZnO}(210 \text{ nm})/(\text{SiO}_2/\text{Ta}_2\text{O}_5)^5$ (sample A), (b) $(\text{Ta}_2\text{O}_5/\text{SiO}_2)^5/\text{ZnO}(219 \text{ nm})/(\text{SiO}_2/\text{Ta}_2\text{O}_5)^5$ (sample B). The incident wavelength was 800 nm.

The calculated transmission spectra are close to the measured transmission spectra, as seen in Fig. 2. This means that it is possible to describe the observed transmission spectra using the optical transfer matrix formalism.

To understand the underlying physics of the enhancement of the nonlinear optical effects, we investigated the spatial distribution of the optical field inside the multilayer structure. The spatial distribution of the optical field can be obtained from the following Helmholtz equation:^{11,12}

$$\nabla^2 \mathbf{E} + \left(\frac{\omega}{c}\right)^2 \varepsilon_r(z) \mathbf{E} = 0, \quad (4)$$

where $\varepsilon_r(z)$ is the relative permittivity as a function of the position. By applying the Helmholtz equation to the multilayer structure, we obtained the spatial distribution of the squared field strength inside the multilayer structure. As shown in Fig. 3(a), the field strength distribution at 800 nm is strongly confined near the defect layer. These results support the use of the ZnO defect-containing photonic crystal to enhance nonlinear optical effects. However, the detuned photonic crystal showed the weak confinement of the optical field, as shown in Fig. 3(b).

Figures 4(a) and 4(b) show the open aperture Z-scan curve of the ZnO defect-containing photonic crystals. In the resonant photonic crystal (sample A), in which the resonant wavelength of the defect mode was adjusted to coincide with the incident laser wavelength, the Z-scan curve exhibited a transmittance dip [Fig. 4(a)]. However, in the detuned photonic crystal (sample B), where the resonance wavelength of the defect mode was slightly detuned from the incident laser wavelength, the Z-scan curve showed a transmittance peak [Fig. 4(b)]. When compared with the Z-scan curve of the ZnO film [Fig. 4(c)], that of the resonant photonic crystal [Fig. 4(a)] exhibited a larger transmittance dip. By applying Eq. (5) (Ref. 8) to the transmittance minima, T_{\min} , of the Z-scan curves, we obtained the nonlinear absorption coefficients, β , of the samples as follows: $\beta = 2.7 \times 10^{-9} \text{ cm/W}$ (ZnO film), $\beta = 15.0 \times 10^{-9} \text{ cm/W}$ (defect-containing photonic crystal—sample A)

$$T_{\min} = \sum_{m=0}^{\infty} \frac{(-q_0)^m}{(m+1)^{3/2}}, \quad (5)$$

where $q_0 = \beta I_0 L_{\text{eff}}$ and I_0 is the intensity of the focused beam, and $L_{\text{eff}} = (1 - e^{-\alpha L}) / \alpha$, with L being the sample thickness. As can be seen in the spatial distribution of the squared field strength inside the multilayer structure (Fig. 3), the spatial distribution of the optical field is strongly confined near the defect layer. The strong confinement of the optical field by the photonic crystal structure increases the nonlinear absorption of the ZnO defect. Therefore, a Z-scan curve of the resonant photonic crystal (sample A) produces a transmittance dip larger than that of the ZnO film. In order to understand quantitatively the enhancement of nonlinear absorption by the confinement of optical field, we introduce an enhancement factor G defined as

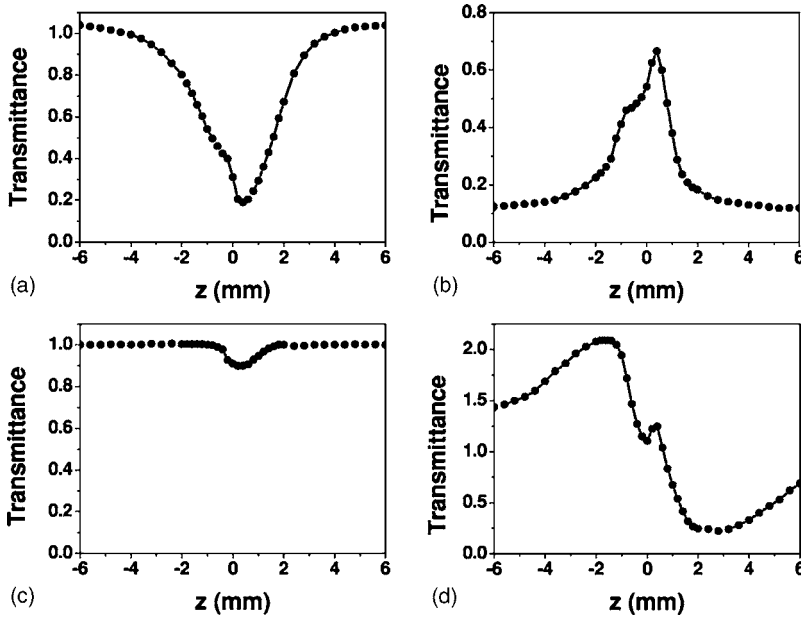


FIG. 4. Open-aperture Z-scan curves of (a) and (b), the ZnO-defect-containing photonic crystals, and (c), 210 nm thick ZnO film: (a) $(\text{Ta}_2\text{O}_5/\text{SiO}_2)^5/\text{ZnO}(210 \text{ nm})/(\text{SiO}_2/\text{Ta}_2\text{O}_5)^5$ (sample A), (b) $(\text{Ta}_2\text{O}_5/\text{SiO}_2)^5/\text{ZnO}(219 \text{ nm})/(\text{SiO}_2/\text{Ta}_2\text{O}_5)^5$ (sample B). The closed aperture Z-scan curve of 210 nm thick ZnO film is shown in (d). Incident wavelength=800 nm, pulse energy=1.6 μJ , pulse duration=130 fs, repetition rate=1 kHz, beam diameter=19.4 μm .

$$G = \frac{1}{d_{\text{defect}}} \int_0^d \frac{|E_{\text{defect}}(z)|^2}{|E_{\text{incident}}|^2} dz, \quad (6)$$

where d_{defect} is the thickness of defect layer, $E_{\text{defect}}(z)$ is the amplitude of field in the defect layer as a function of position z , and E_{incident} is the amplitude of incident field. By applying the spatial distribution of optical field to Eq. (6), we obtained the enhancement factor of 18.4. The ratio of the nonlinear absorption coefficient of the photonic crystal to that of the ZnO film is smaller than the theoretical calculation considering the confinement effect in Fig. 3(a). One possible cause of this discrepancy is that the spectral linewidth (~ 13.0 nm) of femtosecond laser pulse is wider than the bandwidth (~ 7.3 nm) of defect mode in the photonic crystal. According to the optical transfer matrix formalism, the confinement of optical field depends on the incident wavelength. For the resonant photonic crystal, the enhancement factor has the maximum value at the center wavelength of laser pulse. Meanwhile, the enhancement factor decreases in the short or the long wavelength edge. Therefore, the effective value of enhancement factor becomes smaller than the theoretical value by the confinement effect at the resonant wavelength of 800 nm. Another possible reason is that nonlinear refraction can shift the band center of defect mode away from the center wavelength of laser pulse. This detuning would weaken the confinement of optical field near the defect layer. Next, we consider the Z-scan curve of the detuned photonic crystal (sample B). As can be seen in Fig. 4(b), the detuned photonic crystal exhibited saturable absorption with increasing the intensity of incident laser beam. From the transmittance maximum of the Z-scan curve,⁸ we obtained the nonlinear absorption coefficient, β , of the sample as $\beta = -6.6 \times 10^{-9}$ cm/W (defect-containing photonic crystal—sample B). In the detuned photonic crystal, we attributed the saturable absorption to the negative nonlinear refraction of the defect. In the Z-scan experiment using a single ZnO film [Fig. 4(d)], we found the sign of the nonlinear refractivity to be negative. By applying Eq. (7) (Ref. 8)

to the difference between the peak and valley transmittances, ΔT_{pv} , in the closed aperture Z-scan curve, we obtained the nonlinear refractive index, $\gamma = -6.2 \times 10^{-13}$ cm²/W (ZnO film)

$$\Delta T_{\text{pv}} = 0.404(1 - S)^{0.25} |\Delta\Phi_0|, \quad (7)$$

where

$$\Delta\Phi_0 = \gamma(2\pi/\lambda)I_0L_{\text{eff}}.$$

Here, S is the aperture linear transmittance and $\Delta\Phi_0$ is the nonlinear phase shift of the laser beam passed through the sample film. The negative nonlinear refraction pushes the resonance wavelength of the detuned photonic crystal toward the incident laser wavelength. The shift in the resonance wavelength of the defect mode gives the transmittance peak in the Z-scan curve.

IV. CONCLUSIONS

ZnO defect-containing photonic crystals, $(\text{Ta}_2\text{O}_5/\text{SiO}_2)^5/\text{ZnO}/(\text{SiO}_2/\text{Ta}_2\text{O}_5)^5$, were prepared by e-beam deposition and magnetron sputtering, and their transmission spectra revealed a defect mode resonance and a broad photonic band gap. The defect mode resonance occurred near 800 nm: $[\lambda_{\text{peak}}(\text{sample A})=800 \text{ nm}$ and $\lambda_{\text{peak}}(\text{sample B})=810 \text{ nm}]$. The observed transmission spectra could be described by applying the optical transfer matrix formalism to the multilayer structure. When compared with the Z-scan curve of the ZnO film, that of the resonant photonic crystal exhibited a larger transmittance dip. The enhancement of the nonlinear absorption in the resonant photonic crystal was due to the strong confinement of the optical field. Meanwhile, the detuned photonic crystal (sample B) showed saturable absorption with increasing the intensity of incident laser beam. This is attributed to the fact that the negative nonlinear refraction pushes the resonance wavelength of detuned photonic crystal toward the incident laser

wavelength. The shift in the resonance wavelength of the defect mode gives the transmittance peak in the Z -scan curve.

ACKNOWLEDGMENT

This work was supported by the Korea Science and Engineering Foundation (KOSEF) through the Quantum Photonic Science Research Center, Korea.

- ¹P. T. Hsieh, Y. C. Chen, C. M. Wang, Y. Z. Tsai, and C. C. Hu, *Appl. Phys. A: Mater. Sci. Process.* **A84**, 345 (2006).
²M. H. Huang, S. Mao, H. Feick, H. Yan, Y. Wu, H. Kind, E. Weber, R. Russo, and P. Yang, *Science* **292**, 1897 (2001).
³H. Cao, Y. G. Zhao, S. T. Ho, E. W. Seelig, Q. H. Wang, and R. P. H. Chang, *Phys. Rev. Lett.* **82**, 2278 (1999).

- ⁴S. M. Abrarov, S. U. Yuldashev, T. W. Kim, S. B. Lee, H. Y. Kwon, and T. W. Kang, *J. Lumin.* **114**, 118 (2005).
⁵S. P. Lau, H. Y. Yang, S. F. Yu, H. D. Li, M. Tanemura, T. Okita, H. Hayano, and H. H. Hng, *Appl. Phys. Lett.* **87**, 013104 (2005).
⁶J. H. Lin, Y. J. Chen, H. Y. Lin, and W. F. Hsieh, *J. Appl. Phys.* **97**, 033526 (2005).
⁷W. Zhang, H. Wang, K. S. Wong, Z. K. Tang, G. K. L. Wong, and R. Jain, *Appl. Phys. Lett.* **75**, 3321 (1999).
⁸M. Sheik-Bahae, A. A. Said, T. H. Wei, D. J. Hagan, and E. W. Van Stryland, *IEEE J. Quantum Electron.* **26**, 760 (1990).
⁹E. Hecht, *Optics* (Addison-Wesley, Singapore, 1987), Chap. 9.
¹⁰J. Bonse, K. W. Brzezinka, and A. J. Meixner, *Appl. Surf. Sci.* **221**, 215 (2004).
¹¹T. K. Lee, A. D. Bristow, J. Hübner, and H. M. van Driel, *J. Opt. Soc. Am. B* **23**, 2142 (2006).
¹²I. V. Guryev, O. V. Shulika, I. A. Sukhoivanov, and O. V. Mashoshina, *Appl. Phys. B: Lasers Opt.* **B84**, 83 (2006).